sciendo

Environmental & Socio-economic Studies

DOI: 10.2478/environ-2020-0016

Environ. Socio.-econ. Stud., **2020, 8, 3: 34-47**

Original article

Radar reflectivity signatures and possible lead times of warnings for very large hail in Poland based on data from 2007-2015

Wojciech Pilorz [1, 2]*, Ewa Łupikasza[1]

[1]*Institute of Earth Sciences, Faculty of Natural Sciences, University of Silesia in Katowice, Będzińska Str. 60, 41-200 Sosnowiec, Poland*

[2]*Skywarn Poland Association, 29 Listopada Str. 18/19, 00-465 Warsaw, Poland*

*E–mail address (*corresponding author): wojciech.pilorz@gmail.com*

ORCID iD: Wojciech Pilorz: https://orcid.org/0000-0001-9204-0680; Ewa Łupikasza: https://orcid.org/0000-0002-3910-9076

ABSTRACT

Hail involving very large hailstones (maximum diameter ≥ 5 cm), is a rare but very hazardous phenomenon in Poland, and can be forecast using reflectivity signatures. Every year, Poland experiences from one to over a dozen storms with such large hailstones. Despite the current recommendations regarding polarimetric techniques used in hail risk monitoring, Poland does not have a fully polarimetric radar network. Therefore it is essential to check hail detection capabilities using only reflectivity techniques based on individual radar systems involving hail detection algorithms such as Waldvogel et al. (1979) or Vertically Integrated Liquid thresholds connected with manual signature analysis to get better warning decisions. This study is aimed to determine the reflectivity features, thresholds and lead times for nowcasting of severe storms with very large hailstones in Poland, using data from the Polish radar system and from the European Severe Weather Database for the period 2007–2015. Most incidents involving very large hailstones were linked to supercell storms with distinctive reflectivity signatures, however, some storms with extremely large hailstones presented very poorly developed signatures. These signatures enabled the prediction of hail involving very large hailstones approximately 29 minutes before it fell. The Lemon (1980) criterion and WER were found to be the best hail predictors for Polish radar system conditions.

KEY WORDS: reflectivity signatures, meteorological radar, very large hailstones, lead time, Poland

ARTICLE HISTORY: received 20 June 2020; received in revised form 12 August 2020; accepted 24 August 2020

1. Introduction

Severe storms, particularly those involving very large hailstones, are counted among the most hazardous weather phenomena in Central Europe. While knowledge of trends in small-scale severe weather events such as hail or thunderstorms is still insufficient, it is more likely than not that the frequency of the most intense storms will increase substantially in some areas under projected twenty-first century warming (HARTMANN ET AL., 2013). However, wide discrepancies exist regarding the probability of hail in Central Europe. Insufficient monitoring of hail events over the long term has hampered statistical analysis, and thus evidence for changes in these events on a regional scale is insufficient. Most of the studies based on hail observations at weather stations found negative trends in the number of hail days; however, such trends usually lack statistical significance (TWARDOSZ ET AL., 2010, PUNGE & KUNZ, 2016). Irrespective of past trends in hail frequency, the increases in storm intensity projected by climate models may lead to more frequent occurrences of very large hailstones. Accurate forecasting of this kind of hail helps to reduce the damaging effect of this violent weather event. Currently, nowcasting, based on radar data, is the most effective method for the precise prediction of severe weather events. Radar signatures and echo properties associated

with severe thunderstorms have been investigated since the end of World War II, when military radar was first used for meteorological purposes (Stout & Huff, 1953, Tuszyńska, 2011). Several reflectivity signatures have been recognised as effective hailstorm indicators, including Weak Echo Region (WER) (Chisholm & Renick, 1972), hook echo (Stout & Huff, 1953, Fujita, 1973, Markowski, 2002) and Three-Body Scatter Spike/signature (TBSS) (Wilson & Reum, 1986, 1988, Zrnić, 1987, Lemon, 1998).

A significant breakthrough in hail detection research was made by Waldvogel et al. (1979), who proposed the difference between the height of 45 dBZ contours and freezing level as an indicator for hail detection. Knight & Knight (2001) concluded that hailstorm severity depends on the strength of the updraft lifting large accumulations of hydrometeors to high altitudes. This results in a raised Echo Top Height – ETH (the maximum height at which a given reflectivity value is found), high Column Maximum reflectivity - CMAX (maximum reflectivity value within the vertical column of air), and hence high Vertically Integrated Liquid (VIL) parameters. A large accumulation of hydrometeors above the freezing level (0°C isotherm) is a feature of a hail threat and hence 'the 50-dBZ ETH/freezing level difference' is calculated as a hail probability indicator. The 50 dBZ threshold is stricter than that of Waldvogel et al. (1979).

Reflectivity features linked to severe storms with large hailstones have also been identified by Lemon (1980), Witt (1996), Witt et al. (1998), Zrnić & Ryzhkov (1999), Schuster et al. (2006), López & Sánchez (2009), Donavon & Jungbluth (2007), Skripniková & Řezáčová (2014), and Kunz & Kugel (2015). Reflectivity of at least 50 dBZ at a height of 8 km is the threshold for hail risk (Lemon, 1980). When reflectivity at 'low elevation' reaches 60 dBZ, hail is probable (Witt, 1996). Many researchers have reviewed the criterion originally proposed by Waldvogel et al. (1979) and modified the threshold values involved. For example, Witt et al. (1998) developed a Hail Detection Algorithm (HDA) changing the minimal difference of the hail probability to 1.6 km and defining a 5.5 km difference as a 100% probability of hail. While testing numerous techniques, Skripniková & Řezáčová (2014) created their own 'combi-criterion' to determine hail occurrence. A similar study on the assessment of hail detection algorithms was performed by Kunz & Kugel (2015). Donavon & Jungbluth (2007) proved the strong linear dependence of hail on the difference between the freezing level and the top of 50 dBZ reflectivity. Schuster et al. (2006) analysed CAPPI (Constant Altitude Plan Position Indicator) at an altitude of 1.5 km and proposed a reflectivity of 55 dBZ as the threshold for hail risk. López & Sánchez (2009) examined VIL, maximum reflectivity, storm top height, maximum reflectivity height, reflectivity change rate, and the tilt of the storm as hail predictors and identified VIL as a good method for differentiating hailstorms. In recent years, dual-polarisation radar studies with multiple applications constitute the fastest-developing current of radar hail identification (Zrnić & Ryzhkov, 1999, Kumjian & Ryzhkov, 2008). Hail risk assessment has also been based on the presence of overshooting tops (OTs) (e.g. Punge et al., 2017), changes in lightning activity (Wapler, 2017; Farnell et al., 2016), or both (MikušJurković et al., 2015). Some hailstorms may significantly exceed tropopause level (Punge et al., 2017) or contain a high-reflectivity core at high altitudes (Marra et al., 2017).

Currently, nowcasting based on radar data are the most effective methods for the precise prediction of severe hail as well as machine learning including convective parameters using Vertically Integrated Liquid (VIL) (Amburn & Wolf, 1997, Delobbe & Holleman, 2006, López & Sánchez, 2009, Stržinar & Skok, 2018, Stefan & Barbu, 2018), the given echo top height (Delobbe & Holleman, 2006, Stefan & Barbu, 2018), Probability of Hail (POH) (Delobbe & Holeman, 2006, Nisi et al., 2016, Lukach et al., 2017, Trefalt et al., 2018), Probability of Severe Hail (POSH) (Lukach et al., 2017), Maximum Expected Severe Hail Size (MESHS) (Nisi et al., 2016) or forecasting by machine learning (e.g. Czernecki et al., 2019).

Reflectivity signatures and lead time for severe hailstorms (defined as the time elapsed between the first occurrence of a radar reflectivity signature and the time hail begins to fall) have not yet been studied in Poland, except for a case study by Pilorz (2014) who indicated the Lemon (1980) technique as the best for nowcasting of hail involving large hailstones. However, the Polish radar system, consisting of 8 C-band radar installations and covering almost the entire country (Fig. 1), enabled us to perform detailed research on this issue.

Radar system coverage is crucial for the efficient detection of reflectivity signatures. North-eastern Poland is poorly covered by this system, which means that low-located signatures may not be detectable there. Therefore, recognising the capabilities of the Polish radar system in terms of detection of reflectivity signatures is essential for improving their performance as warning systems.

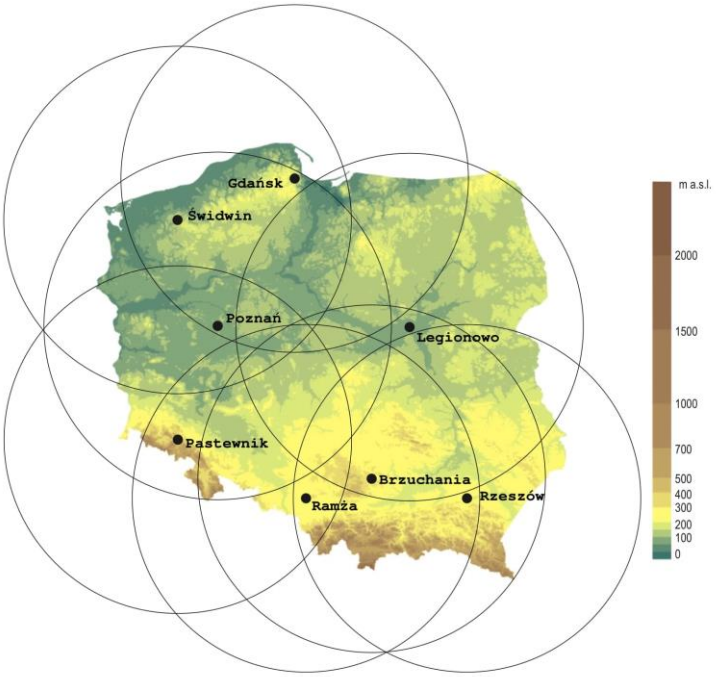

Fig. 1. Polish radar network - POLRAD. black dots – location of the radars. black circles - 250 km radar range

This study identifies the best indicator for a threat of large hailstones in Poland from several reflectivity signatures (see the Data and Methods section). We also analyse lead time for very large hailstones, a subject that has not only not been studied in Poland and has also been rarely analysed abroad (BIERINGER & RAY, 1996; BROTZGE & ERICKSON, 2009). We selected only radar-based indicators which can be rapidly identified without the necessity of sounding data acquisition, since sounding data are available for only three Polish stations (Łeba, Legionowo, Wrocław), all located far from south-eastern Poland where hail occurs most frequently. Sounding data were exceptionally used to find equilibrium levels due to the substantial difference we found between radar-derived and sounding-derived cloud tops.

2. Data and methods

In this article we discuss the reflectivity signatures for the most severe hailstorms that occurred in Poland between 2007 and 2015. Data on their location, time of occurrence, and maximum diameter of hailstones were derived from the European Severe Weather Database (ESWD). The structure, quality control procedures, and applications of the ESWD are discussed in DOTZEK ET AL. (2009). We considered all hailstorms involving at least one observation of hailstones of at least 5 cm in diameter reported to the ESWD at a quality control level of at least QC 0+, which means that the given report was checked and is reliable (DOTZEK ET AL., 2009). Such hailstones not only cause agricultural losses but can also damage automobiles and buildings. In the US, hailstones larger than approximately 25 mm are termed 'severe hail' (PUNGE & KUNZ, 2016). We verified the location and time of each report of very large hailstones (123 cases) using radar data.

The hail reports were assigned to the corresponding storm visible in radar products. We distinguished 69 hailstorms with very large hailstones, of which 7 cases were excluded due to unavailability of radar data or problems with attribution of the hail to a particular storm. In the latter case, the passage of more than one storm was identified over the given coordinates of the fall of hailstones imported from the ESWD. Finally, we analysed the reflectivity signatures for the remaining 62 hailstorms. The radar data are from the Polish radar network (POLRAD) and were provided by the Institute of Meteorology and Water Management – Polish Research Institute (IMGW-PIB). All signatures visible in the radar products were analysed manually. The term 'elevation' refers here to the angle between the antenna tilt and the ground. The data on equilibrium level (the level at which a parcel of buoyant air reaches the same temperature as the surrounding air and becomes stable) was taken from the nearest sounding station, located no more than 200 km from a hailstorm location, provided that it was under the influence of the same air mass, with no front passage. We checked front occurrence using the Deutsche Wetterdienst synoptic charts.

RASMUSSEN & BLANCHARD (1998) admit distances of up to 400 km between sounding station and storm; however, they indicated a sector 150^0 wide (75^0 on each side of the line linking sounding station and storm), depending on the mean wind in the boundary layer. We analysed reflectivity signatures and criteria known to be indicators of hail occurrence, including weak echo region (KNIGHT & KNIGHT, 2001; CHISHOLM & RENICK, 1972), hook echo (DOSWELL & BURGESS, 1993), the LEMON method (1980), the WITT criterion (1996) and three-body spike signature (WILSON & REUM, 1988; LEMON, 1998). We identified the reflectivity signatures first occurring within the radar echo, which thus might be used as an indicator of hailstorm occurrence. Storms that did not include reports of very large hailstones to the ESWD were not analysed; therefore, we did not calculate Heidke Skill Score (HSS) or False Alarm Rate (FAR).

Weak echo region (WER) indicates strong updrafts (KNIGHT & KNIGHT, 2001). Storms involving strong updrafts are more likely to produce severe weather such as hail (MOLLER, 2001). WER indicates the high speed of an air updraft which prevents large hydrometeors from penetrating to the updraft core, so that reflectivity within such a space is low (KNIGHT & KNIGHT, 2001). A weak echo region surrounded by a high reflectivity area from all directions (except inflow region), called a Bounded Weak-Echo Region (BWER), refers to the highest level of storm intensity (MOLLER, 2001). While hook echo, the 'direct result of the mesocyclonic circulation' within a supercell storm (DOSWELL & BURGESS, 1993), does not directly suggest the risk of hail, it does indicate a predisposition to hail occurrence due to the existence of a mesocyclone. FUJITA (1973) identified 5 forms of hook echo, which differ in terms of hook development and reflectivity zone shape. We identified four of these forms among the analysed storms. The LEMON (1980) technique is based on reflectivity at a height of 8 km above ground level (AGL); if this value exceeds 50 dBZ, hail is probable. The method, also known as 50 dBZ Echo Top Height (ETH), assumes that a storm containing a large accumulation of hydrometeors (mainly super-cooled droplets) located high enough above the freezing level is likely to produce large hailstones. Various ranges of air temperature most favourable for hail growth have been identified: from −10 to −25 °C (FOOTE, 1984); from −11 to −19 °C (GRENIER ET AL., 1983); or higher than -19 °C (NELSON, 1983). High reflectivity within these temperature ranges is a significant indicator of hail conditions. We used radar echo vertical cross sections to analyse ETH. WITT'S (1996) criterion involves the presence of high low-elevation reflectivity with a threshold of 60 dBZ as an indicator of the risk of hail (WITT, 1996). In this study, two of the lowest elevations were analysed using the Witt criterion. A Three-body scatter spike/signature (TBSS) is caused by the scattering of a threefold radar beam and its reflection on the large hail core within a storm cell and on the Earth's surface, resulting in a false echo behind the storm. This signature is rare because the echo-free space behind the storm (relating to a radar position) necessary for recognition of the signature is often occupied by the storm's stratiform region. A hail core reflectivity of 60 dBZ (WILSON & REUM, 1988) or 63 dBZ (LEMON, 1998) within a hailstorm is a precondition for TBSS. This signature, when observed in vertical cross sections, is called a flare echo (WILSON & REUM, 1988).

Apart from the best-known signatures described above, we also analysed three parameters based on radar data: 5 dBZ ETH, maximum VIL, and column maximum reflectivity (CMAX). High CMAX values suggest the probability of hail. However, we also noted cases where CMAX values during a storm were lower than 55 dBZ. Generally, the higher the CMAX values attained, the higher the probability of hail. However, the strength of these relationships depends on uncertainties in measurement (SETVÁK ET AL., 2010; see below for details). This dependence also affects VIL, another useful hail detection method (LÓPEZ & SÁNCHEZ, 2009). VIL rises along with the risk of hail; however, as in the case of CMAX, we found several storms with fairly low VIL values.

A strong updraft results in high reflectivity aloft and a high storm top as determined by a 5 dBZ ETH (MOLLER, 2001). In this article we used the threshold of 4 dBZ as the storm top, which is accepted as the echo top estimation algorithm by the Institute of Meteorology and Water Management.

To calculate the lead time we took the time at the beginning of the scan from the radar product as the time of a signature's occurrence. The scanning of the full volume lasts 260 seconds. We estimated the beginning of the fall of very large hailstones based on the lowest-elevation (0.5°) reflectivity analysis. The moment of hail occurrence on the ground was established as the moment when the highest reflectivity value (within a given storm) approached the coordinates of a report of very large hailstones imported from the ESWD. We then compared this time with the time of the first occurrence of the hail signature. This approach enabled us to eliminate inaccuracies between the actual time hail began to fall and the time reported in the ESWD.

Radar measurements may be imprecise. Some uncertainties in reflectivity are possible, especially in its position within the Cartesian 3D field.

VILLARINI & KRAJEWSKI (2010) mentioned the most crucial factors resulting in some false echoes: a) RLAN signals and b) ground clutter (especially from urban and mountain areas). These interferences are eliminated within the POLRAD radar network using Doppler filters, however they leave high uncertainty (JURCZYK ET AL., 2020).

SETVAK ET AL. (2010) listed six reasons for other uncertainties: 1) The radar beam (which determines the top of the reflectivity threshold for an echo top) may be filled by the echo only in the bottom part, while the top is echo-free. Therefore, a wide beam may result in echo top lift as in Fig. 2A. This effect increases along with the radar beam width with increasing distance from the relevant radar site. 2) Reflectivity attenuation by scatterers located closer to the radar than the hailstorm. This may result in a lower value of reflectivity at the top and hence a lower top estimation as well as a lower reflectivity value, as in Fig. 2B. The right supercell is covered by the left supercell, which is closer to the radar, and thus its reflectivity is weaker. Both supercells caused hail at least 7 cm in diameter. 3) Actual atmospheric refraction may differ from the standards accepted for radar reflectivity processing. 4) Some hailstorms located within the range of the radar are affected by a blind spot above the radar. In such cases, the radar scanning strategy did not enable estimation of the echo top for some time. In these situations, we estimated the echo top based on volume scans made at the point that the highest beam was high enough to cover the storm's top. 5) Strong scatterers such as hailstorms can cause false echoes resulting from sidelobe scattering. 6) The interpolation procedure included in the radar data processing algorithm may also lead to false echo distribution artefacts. The described uncertainties affect all hail signatures incorporating the height of a given reflectivity top, particularly high-altitude measurements.

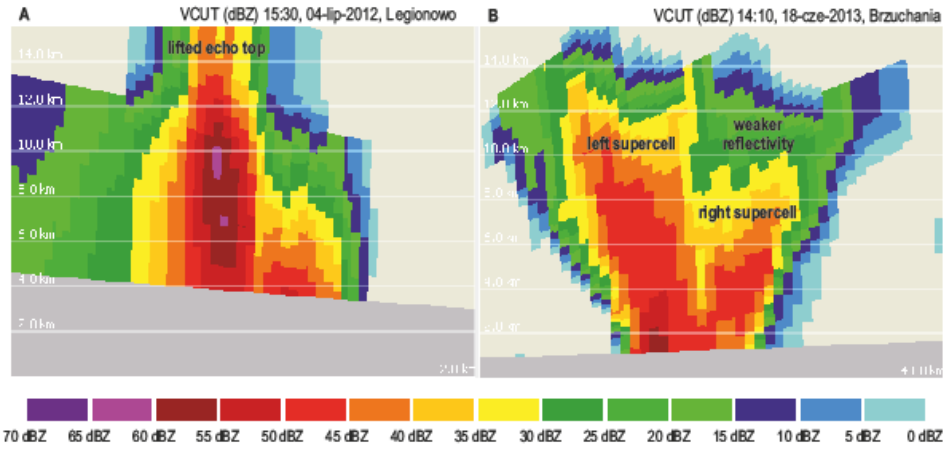

Fig. 2. Examples of the vertical reflectivity distribution with the uncertainties. A - Vertical cross-section through the supercell storm with hailstones of 7 cm in diameter in northern Poland. July 4, 2012 radar Legionowo B - Vertical cross-section through the supercell storms during the splitting process. June 18, 2013 Kielce area, radar Brzuchania

3. Results

3.1. Distribution and statistical characteristics of large and very large hailstones in Poland

Very large hailstones are relatively rare in Poland; therefore we used all ESWD reports (ca 800 reports) on large hailstone (> 2 cm) occurrences to present their spatial distribution as a background for further analysis. Fig. 3 shows the number of large hailstone reports (LHRs) per 1000 km^2 in Poland. Most of lowland Poland reported no more than 3 LHRs per 1000 km^2 between 2007 and 2015. Most of the reports came from southern and eastern Poland (Fig. 3). The maximum density of LHRs exceeded 9 per 1000 km^2 in the central part of southern most Poland. The identified pattern of large hailstone density matches the pattern of annual number of storm days, calculated using data from synoptic stations, as well as lightning density (TASZAREK ET AL., 2015, CZERNECKI ET AL., 2016).

The basic characteristics of very large hailstone occurrence in Poland in the period 2007–2015 are presented in Fig. 4. In terms of time of day, most events occurred between noon (12 UTC) and 6 pm (18 UTC): 58 hailstorms (84% of cases). The hourly maximum of very large hailstone occurrence was noted between 5 and 6 p.m. (17 and 18 UTC) (Fig. 4A). Late morning (10 am to noon, or 10–12 UTC) and evening (6 to 9 p.m., or 18–21 UTC) events each constituted ca 6% of cases

(4 storms with very large hailstones). Only 4% of events were observed at night (midnight to 5 a.m., or 00–05 UTC) (Fig. 4A). In Poland very large hailstones usually form between May and August (Fig. 4B). One of 69 cases was observed in September. However, in 2016, one storm with very large hailstones occurred in the first 10 days of April. Within the very large hailstone category, the largest exceeded 9 cm in diameter (4 hailstorms). The maximum size of hailstones exceeded 7 cm in 16% of cases (Fig. 4C). The frequency of storms involving very large hailstones differed markedly between individual years, from 1 hailstorm in 2014 and 2015 to 15 in 2013 (Fig. 4D). These results, however, may be biased due to underreporting of hailstorms at the beginning of the research period. It is also worth mentioning that 9 storms involving very large hailstones occurred in 2017.

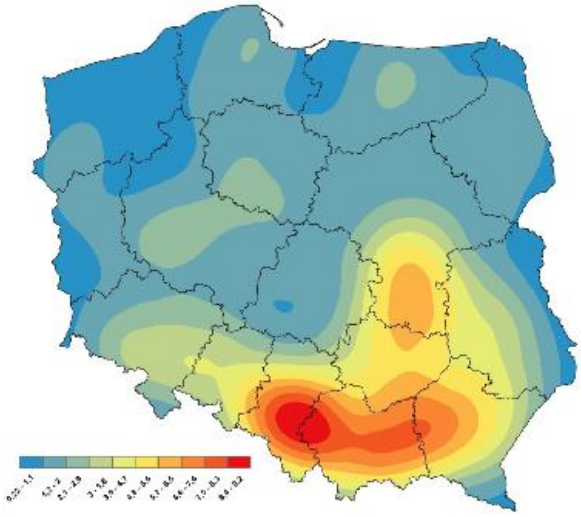

Fig. 3. Large hail distribution in Poland in 2007 – 2015. The colour scale denotes ESWD large hail reports number per 1000 km^2. Map performed using Kernel density estimation. Source: European Severe Weather Database.

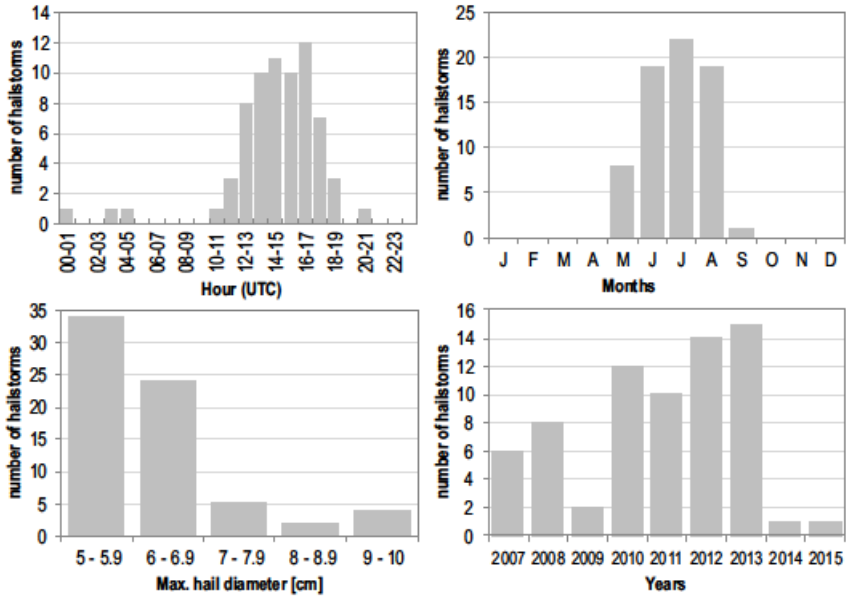

Fig. 4. Basic characteristics of very large hail falls: A – daily course, B – annual course, C – frequency of very large hail falls as a function of maximum hail diameter, D – long-term course

3.2. Reflectivity signatures for hailstorms in Poland

The frequencies of reflectivity signatures and hail detection criteria are presented in Table 1. It is important to note that more than one signature, or criterion, can be identified within the reflectivity for a single storm at a single moment; therefore the total frequency, calculated as the sum of all signature frequencies, exceeds 100%. In such cases both signatures were counted as the first to occur. The fourth and fifth columns of Table 1 include information on how often the signature occurred as the first, thus indicating a threat of hail. The *lead time* column refers to the gap between the moment of the first signature's appearance and the moment very large hailstones began to fall.

Table 1. The frequencies of reflectivity signatures and criteria for 62 hailstorms considered first occurrence" means that given signature appeared as the first hail signal

Signature	Frequency		First occurrence		Average lead time [min]
	No of cases	[%]	No of cases	[%]	
WER/BWER	57	91.9	41	66.1	30
Hook Echo	19	30.6	1	1.6	10
Lemon Technique	59	95.2	42	67.7	27
Witt Criterion	19	30.6	1	1.6	10
TBSS	3	4.8	0	0	-

WER/BWER – Weak Echo Region / Bounded Weak Echo Region, TBSS – Three-Body Scattered Spike

Weak Echo Region. WERs, or BWERs, were the most common signatures, identified in 57 of 62 hailstorms considered (91.9% of cases) (Table 1). Excluding the LEMON (1980) criterion, WER was the most frequent first-occurring signature indicating a potential hail threat. Well-developed BWER for two storms with hailstones measuring 6.0 cm (south-eastern Poland, 5 August 2012) and 8.5 cm in diameter (Katowice, 15 August 2008) are presented in Fig. 5A, B. The distinctive BWER visible in Fig. 5A stretched from the ground to a height of around 6 km. The high reflectivity core surrounding the weak reflectivity area in Fig. 5B is an example of an exceptionally well-developed, partly bounded WER. Fig. 5C, D represents a WER not surrounded by a high reflectivity area, with a vertical extent between 4 and 7 km (Fig. 5). In most storms, the WER signature is not as distinctive as in Fig. 5. The signature sometimes appears at lower levels. Its height and vertical extent depends on weather conditions, especially at equilibrium level height (the level at which a parcel of buoyant air reaches the same temperature as the surrounding air and becomes stable) and CAPE (Convective Available Potential Energy) (MOLLER, 2001). We usually observed WER as a no-echo region at the rear (upwind) part of a storm. In such cases, the high reflectivity core in the proximity of a WER was inclined, as in Fig. 6B, in which the echo-free space below the upper part of this inclined core indicates that the core was upheld by a strong updraft. We also observed a strong contrast in the vicinity of the reflectivity core. In north-eastern Poland, low-located WERs were impossible to detect due to the high elevation of the lowest beam. However, in most hailstorms, WER was easily detectable.

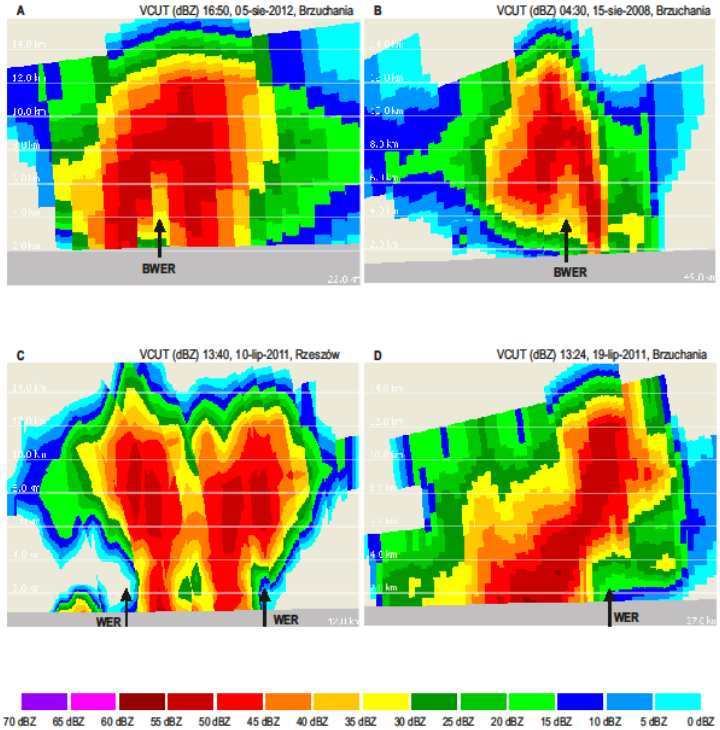

Fig. 5. Radar reflectivity cross-sections with the distinctive BWER (A and B) and WER (C and D) signatures. Time in UTC. Arrows denotes updraft location. A – RM (Right Moving) supercell storm with 6 cm hailstones in south eastern Poland, radar Brzuchania, August 5, 2012, B – the storm in Katowice in August 15, 2008 with hail 8,5 cm in diameter, radar Brzuchania, C – two supercell storms with hailstones up to 6 cm in diameter during the splitting process, radar Rzeszów, July 10, 2011 and D – RM supercell storm with 6 cm hailstones in south eastern Poland, radar Brzuchania, July 19, 2011, Source: IMGW-PIB

Hook echo. The hook echo signature was found in 19 of 62 storms analysed; however, it constituted the first occurring signature for only one hailstorm (Table 1). This suggests that the hook echo is a poor indicator for large hailstone warnings. Typical radar reflectivity distribution for a supercell storm at the lowest elevation (0.5° PPI) and its vertical profile throughout the mesocyclone, manifesting itself as a BWER, is presented in Fig. 6, which also includes the hook echo at the lowest elevation surrounding the echo-free zone of the storm inflow, leading to an updraft seen as a BWER (Fig. 6A). In 34 cases, although we did not find a hook echo signature, the storm's trajectory suggested a supercell; therefore we cross-sectioned the rear (upwind) side of the storm, where the updraft of a supercell storm is located. If the supercell was barely visible or embedded in a larger convective system, we checked numerous profiles to find WER.

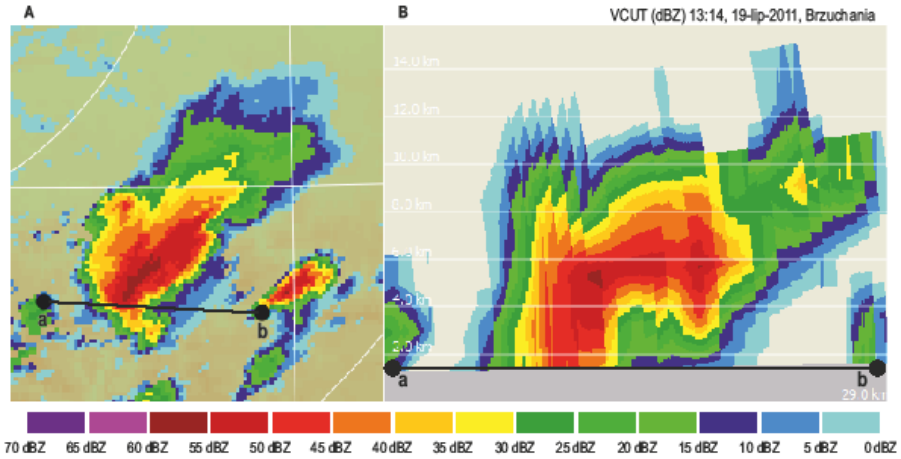

Fig. 6. Reflectivity distribution for the supercell with a hook echo near Tarnów (left picture - the PPI 0.5^0 product, right picture - the vertical cross-section), July 19, 2011, radar Brzuchania, the black line on the PPI denotes the place of the cross-section

Hail detection using the Lemon technique. Reflectivity exceeded 50 dBZ at a height of 8 km (LEMON, criterion) in 59 out of 62 analysed hailstorms. Thus the criterion was not met in only 3 cases, one of which is presented in Fig. 2. The radar beam intercepting this particular left-moving (LM) supercell was weakened by a right-moving (RM) supercell (with hailstones of 9.5 cm in diameter) located closer to the radar. The Lemon criterion was the first signal of a large-hailstone threat in 42 cases (Table 1) and was the first-occurring storm signature in 20 cases. In some cases the 50 dBZ core significantly exceeded the Lemon criterion (8 km AGL). The highest detected level with the 50 dBZ core exceeded 14 km, directly above the WER (Fig. 7A). We estimated the mean 50 dBZ ETH at 10.6 km. For a storm with CMAX lower than 50 dBZ, the lowest 50 dBZ ETH was 0 km. Fifty per cent of 50 dBZ ETH values fell between 9.5 and 12 km, while the maximum value reached 15 km. This extreme case occurred within a supercell storm with hailstones measuring 6.5 cm in the Sandomierz area on 12 June 2010 (Fig. 7A), with the storm top (5 dBZ Echo Top Height) reaching 18 km.

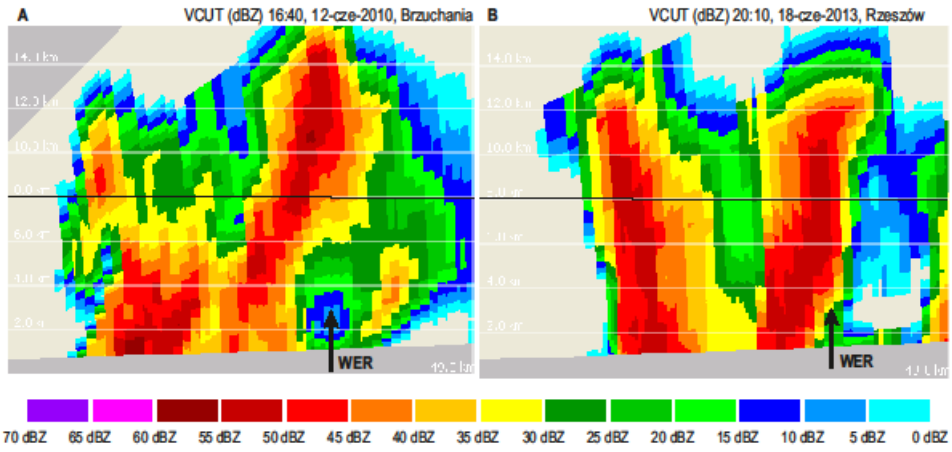

Fig. 7. Vertical cross-sections of the supercell storms. A – RM supercell storm near Sandomierz with hail up to 6,5 cm in diameter. Radar Brzuchania, June 12, 2010 and B - Vertical cross-section through the supercell storms during the splitting process. June 18, 2013 south-eastern Poland. Two storms met Lemon criterion. Slight WER was also visible. Black line denotes the height of 8 km

Hail detection with the Witt criterion. The Witt criterion was met by 19 hailstorms, for which reflectivity exceeded 60 dBZ at the two lowest elevations. However, the Witt criterion was the first-occurring signature, indicating hail risk, for only one hailstorm. For this hailstorm the Witt criterion co-occurred with WER and the Lemon criterion (Table 1), suggesting that high reflectivity appears in the lower troposphere later than WER and high reflectivity aloft. This is characteristic of the hailstorm formation process with a strong updraft appearing first, causing a large number of cloud particles to be lifted to high altitudes, well above the freezing level where the hail forms. Finally, when the hail is large enough to overcome the updraft force, it falls to the Earth's surface (KNIGHT & KNIGHT, 2001), causing higher reflectivity at low elevations. The Witt criterion can therefore be used as a detection method for the fall of hail at the time of observation, rather than as a warning prior to the fall of hail.

Three-Body Scattered Spike. The TBSS signature was identified for 3 storms with very large hailstones. In none of these cases was TBSS the first hail signature; moreover, it did not appear until the hail fell, or even several minutes later. We found two more examples of TBSS; however, one was associated with a hailstorm over Slovakia and the other for a storm involving hailstones smaller than the adopted threshold of 5 cm. The rare occurrence of TBSS eliminated it as a useful indicator for an operational warning system. Therefore TBSS may serve only as a supportive signature. Two cases of three-body scatter are presented in Figs. 8, 9.

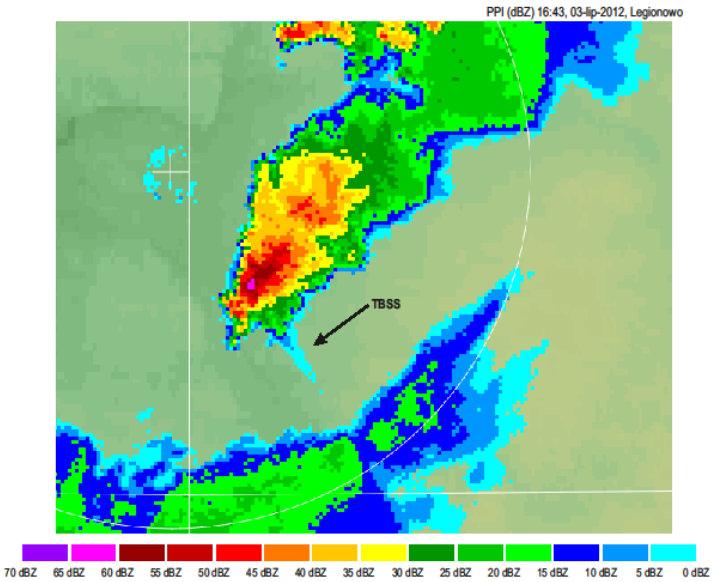

Fig. 8. PPI (10^0 antenna tilt) of the supercell storm in eastern part of Warsaw. TBSS signature is visible at the back side of the storm (according to the radar location). July 3rd, 2012, radar Legionowo

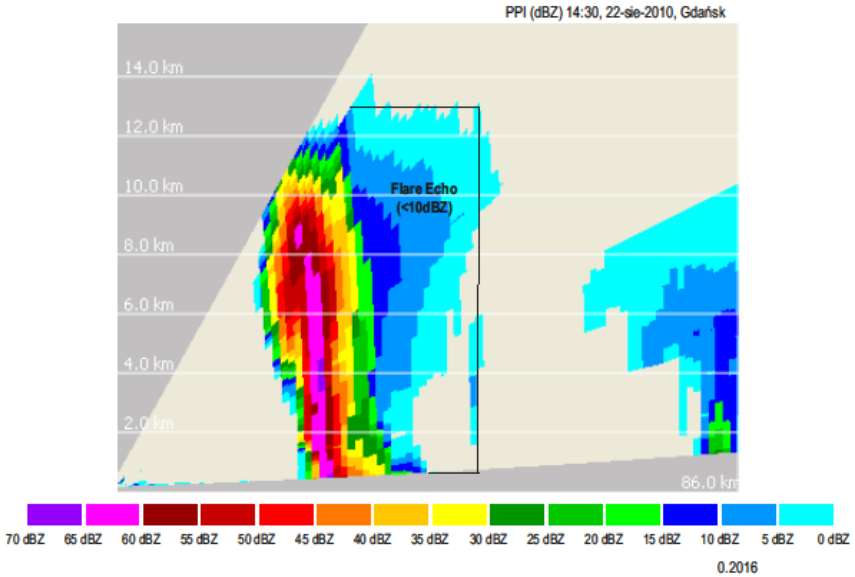

Fig. 9. Vertical cross-section of the RM supercell storm with a 5 cm hailstones in Gdańsk region with the distinctive flare echo. August 22nd, 2010, radar Gdańsk

The TBSS seen in the 10° antenna tilt PPI product (Fig. 8) is related to a storm in Warsaw on 3 July 2012 with a core reflectivity of 65.5 dBZ and hailstones up to 6.5 cm in diameter. The other distinctive TBSS was identified within the supercell storm west of Gdańsk on 22 August 2010 (Fig. 9). The cross section of the Gdańsk storm shows a flare echo at several elevations – from $0{,}5^0$ to a height of 9 km – where reflectivity exceeded 60 dBZ (Fig. 9). In other cases, flare echoes were observed at a maximum of 3 elevations.

3.3. Other reflectivity characteristics

In addition to the best-known signatures described above, we analysed other basic reflectivity characteristics associated with hailstorms (CMAX, VIL, differences between the freezing level and 50 dBZ ETH) which can be identified on the basis of the single-polarisation Polish radar system. The average CMAX for all hailstorms was 59.6 dBZ; 50% of values fell between 57.5 and 62.5 dBZ (Table 2). Minimum and maximum CMAX reached 47.5 dBZ and 68.5 dBZ, respectively, the latter was found within a supercell moving through the Upper Silesia region with hailstones 6.5 cm in diameter. Maximum reflectivity was higher than 65 dBZ for only 5 hailstorms, lower than 50 dBZ for only one.

VIL values, indicating precipitable water suspended in the atmosphere, varied widely between hailstorms with similar maximum hailstone diameters. The average VIL for the analysed hailstorms was 39.5 dBZ, while extremes reached 18 dBZ and 93 dBZ. The 5 dBZ ETH value indicating the storm cloud top was 15.2 km on average and, in the case of 50% of storms with severe hail, between 14 and 16 km (Table 2). The extreme heights for this parameter were 20 (maximum) and 10 km (minimum). Uncertainties concerning these findings are discussed in section 2, 'Data and Methods'.

Table. 2 Selected radar echo characteristics within the 62 analysed hailstorms in Poland in 2007 – 2015

Indicator	CMAX[dBZ]	50 dBZ Echo Top Height [km]	Max. VIL [dBA]	5 dBZ ETH [km]
Min.	47.5	0	18.0	10.0
25th percentile	57.5	9.5	2.5	14.0
Avg.	59.6	10.6	39.5	15.2
75thpercentile	62.5	12.0	48.0	16.0
Max.	68.5	15.0	93.0	20.0

CMAX – column maximum reflectivity within the given hailstorm VIL - Vertically Integrated Liquid within the given hailstorm, Min. – Minimum value of the given feature within the given hailstorm Max. - Maximum value of the given feature within the given hailstorm

As previously mentioned, the accumulated volume of hydrometeors located above the freezing level is crucial for large hailstone formation. Therefore, we calculated the differences between the freezing level and the 50 dBZ ETH. The average difference equalled 7.2 km, indicating a large aggregation of hydrometeors above the freezing level. The difference for 100% large hailstone probability was 5.5 km (WITT, 1998), demonstrating the high degree of utility of the 50 dBZ ETH criterion for detection of the occurrence of very large hailstones in Poland. What is more, WITT (1998) based his algorithm on the 45 dBZ ETH. The large difference between the 50 dBZ ETH and freezing level is due to inclusion in the analysis of larger hailstones than in the case of WITT (1998).

Only one storm was characterised by a reflectivity lower than 50 dBZ; therefore the minimum value of the 50 dBZ ETH was 0 km. Excluding this case, the average for this criterion equalled 10.6 km. The maximum 50 dBZ ETH reached 15 km. This extreme case occurred in a supercell storm with hailstones measuring 6.5 cm in the Sandomierz area on 12 June 2010 (Fig. 7A), when the 5 dBZ ETH reached 18 km. The recognised maximum 5 dBZ ETH was 20 km, measured on 11 June 2010 in north-western Poland within a supercell storm with a high level of precipitation including very large hailstones. The mean value of the 5 dBZ ETH was 15.2 km, substantially higher than the highest equilibrium levels we found in the proximity of the analysed hailstorms. The difference between the 5 dBZ ETH and the height of the equilibrium level (which are usually quite similar) was partially due to the overshooting tops present within the storms, which included strong updrafts. This may also result from possible uncertainties in radar measurements, as discussed in section 2, 'Data and Methods', or from radiative cooling of the cloud top (EBERT & HOLLAND, 1992). The VIL values differed strongly, depending on the hailstorm (Table 2); thus this parameter is not helpful in Polish conditions. We also observed high VIL values for storms that did not involve very large hailstones. Therefore, VIL is potentially affected by a high number of false alarms. Basically, there is no

guarantee that a storm with relatively low reflectivity, and hence low VIL, will produce smaller hailstones than one with relatively high reflectivity. Increases in VIL and other parameters cause increases in hail diameter; however, large-diameter hail is also possible at low VIL, and the converse is also true.

3.4. Lead time

The mean lead time for all hailstorms, estimated mostly based on WER and the Lemon hail detection technique, equalled 29 minutes (Table 1). Hook echo and the WITT (1996) criterion were also first-occurring signatures, but only for two hailstorms. Moreover, they co-occurred with WER and Lemon signatures. Details concerning lead times are presented in Table 1. Lead times ranged from 30 minutes after (negative lead time) to 100 minutes before the first fall of very large hailstones. In two cases, the signatures appeared after the first fall of very large hailstones (negative lead time) and in 5 other cases they appeared at the time of the fall (lead time = 0). Lead times between 0 and 10 minutes and between 11 and 30 minutes were found in 13 (21%) and 21 (34%) hailstorms, respectively. Lead times longer than 30 minutes were found in 25 hailstorms (40%). The most frequent lead time was between 15 and 35 minutes (28 hailstorms); in the case of 10 hailstorms (16%) it was longer than 45 minutes (Fig. 10).

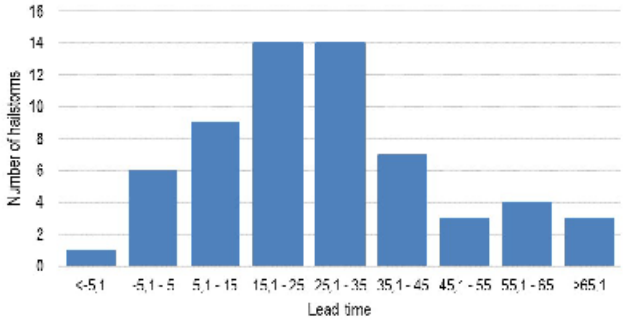

Fig. 10. The number of hailstorms with the given lead time

It should be stressed that we estimated the lead time for the fall of very large hailstones. It is possible that a fall of large hailstones occurred prior to the fall of very large hailstones. The established lead times were long enough to announce a very large hailstone warning for most storms. We investigated whether the poorer radar coverage in the northern part of Poland resulted in weaker visibility of low-located signatures and thus delayed signature recognition. Therefore we divided Poland into northern and southern parts; the division line was the 52nd parallel. We calculated average lead time for northern Poland as 26 minutes (13 hailstorms), and for southern Poland as 30 minutes (48 hailstorms).

3.5. Types of hailstorms

Supercell storms have unique reflectivity features, such as hook echo, and slightly different directions of movement compared with non-supercell storms. We used these features, particularly a supercell's specific trajectory, to distinguishing between supercell and non- supercell storms producing hail. Supercellular features were identified in 53 out of 62 hailstorms (85.5%). In some cases, hailstorm trajectories were changed slightly, making it difficult to assess whether the storm was a supercell or not. We called such cases 'possible supercell storms'. Possible supercellular features were identified in 5 hailstorms. These two categories involved 93.5% of all analysed hailstorms. Four hailstorms had no supercellular features. Storms sometimes undergo a process of cell splitting, spawning two supercells: one left-moving (LM), the other right-moving (RM). We distinguished 38 RM and 13 LM supercells. The splitting process was observed in 30 hailstorms. In one case, hail was followed by the splitting process. The domination of supercells among storms producing very large hailstones confirmed the results reported by DOSWELL (2001). We found an average maximum hail diameter of 6.04 cm for RM and 6.19 cm for LM supercells.

4. Discussion

This study aimed at the identification of radar reflectivity signatures and criteria useful for warnings concerning the fall of very large hailstones in Poland. Our research is based on the European Severe Weather Database (ESWD), which enabled us to analyse combined observational, radar, and ESWD data, particularly lead-time analysis for very large hailstones. Several problems associated with data quality and interpretation which occurred during our research need to be discussed. The ESWD data may be affected by under-reporting of hail, especially before 2010, due to the weak involvement of ESWD management and Skywarn Poland members in reporting severe weather at that time. It is also possible that hailstones larger than 50 mm co-occurred with hailstones of 35–49 mm, but were not reported, or even recorded, in cases where they appeared in uninhabited areas.

Moreover, some degree of subjectivity is involved in the assessment of certain weakly-developed signatures such as WER or hook echo. This may

impact lead time and thus the effectiveness of hail warning. However, the average lead time we calculated for very large hail (29 minutes) was long enough to issue a warning even given a delayed identification of the signature. Such problems are inevitable in the interpretation of radar reflectivity measurements. Even when a signature is correctly identified, a warning may not always be issued due to the time required for human interpretation of the signature. The time scale of signature interpretation may also depend on the individual forecaster. Moreover, a storm of brief duration may lack some reflectivity signatures due to the short time between its mature and dissipating stages. This concerns the rare low-level hook echo signature occurring only relatively close to the radar site and requiring a low-located radar beam. WER signatures are formed by a strong updraft, which is a storm-productive factor; therefore WER appears more frequently than hook echo.

A high ETH exceeding the tropopause level within hailstorms in Poland was also reported for a severe hailstorm in Italy where reflectivity up to 55 dBZ reached 12 km AGL (MARRA ET AL., 2017). Some studies have also indicated that a cloud can develop above the tropopause level. For example, PUNGE ET AL. (2017) found that, in Poland, the coldest cloud top for hailstorms is usually 2–7 °C colder than the tropopause level.

A lead time of 29 minutes for hail in Poland is longer than the interval obtained by WAPLER (2017) based on lightning jump data and mesocyclone detection. Using TBSS, LEMON (1998) found a warning lead time of 10–30 minutes for hailstones equal to, or greater than, 2.5 cm in diameter. We found that in Poland more than 85% of falls of very large hailstones were clearly related to supercell storms. WAPLER (2017) found that in Germany, nearly 75% of hailstorms were associated with supercells identified by radar mesocyclone detection. KNIGHT & KNIGHT (2001) also indicated supercells as the most hail-producing storm type due to the mesocyclone, i.e. the strong updraft which creates numerous hail cycles within the storm. The strength of the updraft determines the amount of water lifted above the freezing level where hailstones form (KNIGHT & KNIGHT, 2001). The formation of large hailstones requires a great deal of lifted water; thus a strong updraft explains the great difference between the freezing level and the 50 dBZ ETH we observed.

A strong updraft generates an overshooting top and consequently high values of storm tops; it also leads to a high ETH for the given reflectivity values (MOLLER, 2001). The 9 cases (14%) with no supercell storms were problematic due to the following reasons: a hailstorm was embedded in a larger convective system; there was no difference between hailstorm movement and the movement of other storms; a hailstorm occurred far from a radar site, which may have distorted the storm's shape and movement. Some of these storms might have been supercells that went unrecognised due to limitations in movement criteria.

Our results proved that the appearance of a signature depends on the distance between the storm and the radar. In eastern Poland, located farthest from the radar, the radar beam runs high, which results in missing low-located signatures such as the WITT (1996) criterion and hook echo. A high radar beam location also influences the correctness of WER identification within low-topped storms. Such storms are characterised by low-located signatures which are impossible to identify at great distances from the radar source. Nevertheless, in north-eastern Poland, where the lowest radar beam is characterised by a relatively high altitude, we were able to identify signatures for most hailstorms. The high altitude of the lowest radar beam may play a role in certain individual cases, especially in the case of low-topped storms. This problem is crucial for the issue of operational warnings based on the inadequate Polish radar system.

The major uncertainty is a lack of no hail presence information sources. ESWD proves only information about the hail on the ground, but for false alarm rate calculating we also need information about no hail at the given point. Thus checking the above mentioned techniques for operational purposes is impossible. Moreover, manual, real-time hail forecasting is ineffective and may lead to omissions in some cases.

5. Conclusions

Our results indicate that the Lemon technique with weak echo region is the best hail detection method for use within the Polish radar system. The Lemon criterion also constituted the highest percentage of first-occurring signatures, followed by WER. Lead times estimated by the Lemon technique were similar to those for WER, reaching 29 minutes. All hailstorms were characterised by significant differences between freezing level and 50 dBZ ETH. Thus the algorithms of hail detection based on such differences, e.g. HDA or WALDVOGEL ET AL. (1979), should also be suitable for hail risk assessments. The trajectory analysis indicated that the great majority, in fact, nearly all, of the hailstorms were supercell storms, most of which

were right-moving. Taking these facts into account, in favourable conditions (TASZAREK ET AL., 2017; GROENEMEIJER & VAN DELDEN, 2007) the occurrence of a supercell itself should be treated as an indicator for a very large hailstone warning.

Acknowledgements

All of the radar data on which this investigation is based were kindly provided by the Polish Institute of Meteorology and Water Management. We thank Irena Tuszyńska and Jan Szturc for their supportive comments on the Polish radar system products. We express our special thanks to individuals submitting reports to the European Severe Weather Database, especially Artur Surowiecki and Igor Laskowski of the Skywarn Poland Association. Supportive comments by an anonymous reviewer are also appreciated.

This research did not receive any specific grant from funding agencies in the public, commercial, or not-for-profit sectors.

References

Amburn S.A., Wolf P. L. 1997. VIL Density as a Hail Indicator. *Weather and Forecasting*, 12: 473–478.

Bieringer P., Ray P.S. 1996. A Comparison of Tornado Warning Lead Times with and without NEXRAD Doppler Radar. *Weather and Forecasting*, 11: 47–52.

Brotzge J., Erickson S. 2009. NWS Tornado Warnings with Zero or Negative Lead Times. *Weather and Forecasting*, 24: 140–154.

Chisholm A.J., Renick J.H. 1972. The kinematics of multicell and supercell Alberta hailstorms. Alberta hail studies 1972. *Research Council of Alberta Hail Studies Report*, 72, 2: 24–31.

Czernecki B., Taszarek M., Kolendowicz L., Konarski J. 2016. Relationship between human observations of thunderstorms and the PERUN lightning detection network in Poland. *Atmospheric Research*, 167: 118–128.

Czernecki B., Taszarek M., Marosz M., Kolendowicz L., Półrolniczak M., Wyszogrodzki A., Szturc J. 2019. Application of machine learning to large hail prediction – the importance of radar reflectivity, lightning occurrence and convective parameters derived from ERA5. *Atmospheric Research*, 227, 1: 249–262.

Delobbe L., Holleman I., 2006. Uncertainties in radar echo top heights used for hail detection. *Meteorological Applications*, 13: 361–374.

Donavon R.A., Jungbluth K.A, 2007. Evaluation of a Technique for Radar Identification of Large Hail across the Upper Midwest and Central Plains of the United States. *Weather and Forecasting*, 22: 244–254.

Doswell C.A. 2001. Severe Convective Storms – An Overview. [in:] C.A. Doswell (Eds.) *Severe Convective Storms*, American Meteorological Society, Boston: 1–26.

Doswell C.A., Burgess D.W. 1993. Tornadoes and tornadic storms: A review of conceptual models. [in:] C. Church, D. Burgess, C.A. Doswell, R. Davies-Jones (Eds.) The Tornado: Its Structure, Dynamics, Prediction and Hazards. *Geophysical Monograph Series*, 79, American Geophysical Union: 161–172.

Dotzek N., Groenemeijer P., Feuerstein B., Holzer A.M. 2009. Overview of ESSL's severe convective storms research using the European Severe Weather Database ESWD. *Atmospheric Research*, 93: 575–586.

Ebert E.E., Holland G.J. 1992. Observations of record cold cloud-top temperatures in tropical cyclone Hilda (1990). *Monthly Weather Review*, 120, 10: 2240–2251.

Farnell C., Rigo T., Pineda N. 2016. Lightning jump as a nowcast predictor: Application to severe weather events in Catalonia. *Atmospheric Research*, 183: 130–141.

Foote G.B. 1984. A study of hail growth utilizing observed storm conditions. *Journal of Applied Meteorology and Climatology*, 23: 84–101.

Fujita T. 1973. Proposed mechanism of tornado formation from rotating thunderstorms. *Proceedings 8th Conference on Severe Local Storms, 15–17 Oct. 1973*, Boston, US.

Grenier J.C., Admirat P., Zair S. 1983. Hailstone growth trajectories in the dynamic evolution of a moderate hailstorm. *Journal of Applied Meteorology and Climatology*, 22: 1008–1021.

Groenemeijer P.H., Van Delden A. 2007. Sounding-derived parameters associated with large hail and tornadoes in the Netherlands. *Atmospheric Research*, 83: 473–487.

Hartmann D.L., Klein Tank A.M.G., Rusticucci M., Alexander L.V., Brönnimann S., Charabi Y., Dentener F.J., Dlugokencky E.J., Easterling D.R., Kaplan A., Soden B.J., Thorne P.W., Wild M., Zhai P.M 2013. Observations: Atmosphere and Surface. [in:] T.F. Stocker, D. Qin, G.-K. Plattner, M. Tignor, S.K. Allen, J. Boschung, A. Nauels, Y. Xia, V. Bex, P.M. Midgley (Eds.) *Climate Change 2013: The Physical Science Basis. Contribution of Working Group I to the Fifth Assessment Report of the Intergovernmental Panel on Climate Change*. Cambridge University Press, Cambridge, UK and New York, NY, USA.

Jurczyk A., Szturc J., Otop I., Ośródka K., Struzik P. 2020. Quality-Based Combination of Multi-Source Precipitation Data. *Remote Sensing*, 12(11), 1709.

Knight C.A., Knight N.C. 2001. Hailstorms. [in:] Doswell, C.A. (Eds.), *Severe Convective Storms.* American Meteorological Society, Boston: 223–254.

Kumjian M.R., Ryzhkov A.V. 2008. Polarimetric Signatures in Supercell Thunderstorms. *Journal of Applied Meteorology and Climatology*, 47: 1940–1961.

Kunz M., Kugel P.I.S. 2015. Detection of hail signatures from single-polarization C-band radar reflectivity. *Atmospheric Research*, 153: 565–577.

Lemon L.R. 1980. *Severe thunderstorms radar identification techniques and warning criteria: A preliminary report*. NOAA Tech. Memo.

Lemon L.R. 1998. The Radar "Three-Body Scatter Spike": An Operational Large-Hail Signature. *Weather and Forecasting*, 13: 327–340.

Lopez L., Sanchez J.L. 2009. Discriminant methods for radar detection of hail. *Atmospheric Research*, 93: 358–368.

Lukach M., Foresti L., Giot O., Delobbe L. 2017. Estimating the occurrence and severity of hail based on 10 years of observations from weather radar in Belgium. *Meteorological Applications*, 24: 250–259.

Markowski P.M. 2002. Hook echoes and Rear-Flank Downdrafts: A Review. *Monthly Weather Review*, 130: 852–876.

Marra A.C., Porcu F., Baldini L., Petracca M., Casella D., Dietrich S., Mugnai A., Sano P., Vulpiani G., Panegrossi G. 2017. Observational analysis of an exceptionally intense hailstorm over the Mediterranean area: Role of GPM Core observatory. *Atmospheric Research*, 192: 72–90.

MikusJurkovic P., StrelecMahovic N., Pocakal D. 2015. Lightning, overshooting top and hail characteristics for strong convective storms in Central Europe. *Atmospheric Research*: 161–162, 153–168.

Moller A.R. 2001. Severe Local Storms Forecasting. [in:] C.A. Doswell (Eds.) *Severe Convective Storms*. American Meteorological Society, Boston: 433–480.

Nelson S.P., 1983. The influence of storm flow structure on hail growth. *Journal of the Atmospheric Sciences*, 40: 1965–1983.

Nisi L., Martius O., Hering A., Kunz M., Gremann U. 2016. Spatial and temporal distribution of hailstorms in the Alpine region: a long-term, high resolution, radar-based analysis. *Quarterly Journal of the Royal Meteorological Society*, 142, 697: 1590–1604.

Pilorz W. 2014. Radarowa detekcja superkomórek burzowych w Polsce. *Teledetekcja Środowiska*, 51: 93–105.

Pilorz W., Laskowski I., Łupikasza E. Taszarek M. 2016. Wind Shear and the Strength of Severe Convective Phenomena—Preliminary Results from Poland in 2011–2015. *Climate*, 4, 51.

Punge H.J., Bedka K.M., Kunz M., Reinbold A. 2017. Hail frequency estimation across Europe based on a combination of overshooting top detections and the ERA – INTERIM reanalysis. *Atmospheric Research*, 198: 34–43.

Punge H.J., Kunz M. 2016. Hail observations and hailstorm characteristics in Europe: A review. *Atmospheric Research*: 176–177, 159–184.

Rasmussen E.N., Blanchard D.O. 1998. A Baseline Climatology of Sounding-Derived Supercell and Tornado Forecast Parameters. *Weather and Forecasting*, 13: 1148–1164.

Schuster S.S., Blong R.J., McAneney K.J. 2006. Relationship between radar derived hail kinetic energy and damage to insured buildings for severe hailstorms in Eastern Australia, *Atmospheric Research*, 81: 215–235.

Setvak M., Lindsey D.T., Novak P., Wang P.K., Radova M., Kerkmann J., Grasso L., Su S.-H., Rabin R.M., Staska J., Charvat Z. 2010. Satellite-observed cold-ring-shaped features atop deep convective clouds. *Atmospheric Research*, 97: 80–96.

Skripniková K., Řezáčová D. 2014. Radar-based hail detection. *Atmospheric Research*, 144: 175–185.

Stefan S., Barbu N. 2018. Radar-derived parameters in hail-producing storms and the estimation of hail occurrence in Romania using a logistic regression approach. *Meteorological Applications*, 25: 614–621.

Stout G.E., Huff F.A. 1953. Radar records Illinois tornado genesis. *Bulletin of the American Meteorological Society*, 34, 281–284.

Stržinar G., Skok G. 2018. Comparison and optimization of radar-based hail detection algorithms in Slovenia. *Atmospheric Research*, 203: 275–285.

Taszarek M., Brooks H.E., Czernecki B. 2017. Sounding-Derived Parameters Associated with Convective Hazards in Europe. *Monthly Weather Review*, 145: 1511–1528.

Taszarek M., Czernecki B., Kozioł A. 2015. A Cloud-to-Ground Lightning Climatology for Poland. *Monthly Weather Review*, 143: 4285–4304.

Trefalt S., Martynov A., Barras H., Besic N., Hering A.M., Lenggenhager S., Notie P., Röthlisberger M., Schemm S., Germann U., Martius O. 2018. A severe hail storm in complex topography in Switzerland – Observations and processes. *Atmospheric Research*, 209: 76–94.

Tuszyńska I. 2011. *Charakterystyka produktów radarowych*. Instytut Meteorologii i Gospodarki Wodnej – Państwowy Instytut Badawczy, Warszawa.

Twardosz R., Niedźwiedź T., Łupikasza E. 2010. Hail thunderstorms in Kraków and their circulation determinants (1863–2008). [in:] T. Ciupa, R. Suligowski (Eds.) *Woda w badaniach geograficznych*. Instytut Geografii Uniwersytet Jana Kochanowskiego, Kielce: 295–305.

Villarini G., Krajewski W.F. 2010. Review of Different Sources of Uncertainty in Single Polarization Radar-Based Estimates of Rainfall. *Survey in Geophysics,* 31: 107–127.

Waldvogel A., Federer B., Grimm P. 1979. Criteria for the Detection of Hail Cells, *Journal of Applied Meteorology and Climatology*, 18: 1521–1525.

Wapler K. 2017. The life-cycle of hailstorms: Lightning, radar reflectivity and rotation characteristics. *Atmospheric Research*, 193: 60–72.

Wilson J.W., Reum D. 1986. „The hail spike": a reflectivity and velocity signature. *Proceedings 23rd Conference on Radar Meteorology*, *22–26 Sep. 1986*, American Meteorological Society, Snowmass, US.

Wilson J.W., Reum D. 1988. The flare echo: Reflectivity and velocity signature. *Journal of Atmospheric and Oceanic Technology*, 5: 197–205.

Witt A. 1996. The relationship between low-elevation WSR-88D reflectivity and hail at the ground using precipitation observations from the VORTEX project. *Proceedings 18th Conference on Severe Local Storms, 19–23 Feb. 1996*, San Francisco, US: 183–185.

Witt A. 1998. An Enhanced Hail Detection Algorithm for the WSR-88D. *Weather and Forecasting*, 13: 286–303.

Zrnić D.S. 1987. Three-body scattering produces precipitation signature of special diagnostics signature. *Radio Science*, 22: 76–86.

Zrnić D.S., Ryzhkov A.V. 1999. Polarimetry for Weather Surveillance Radars. *Bulletin of the American Meteorological Society*, 80: 389–406.